

FID-A133 552

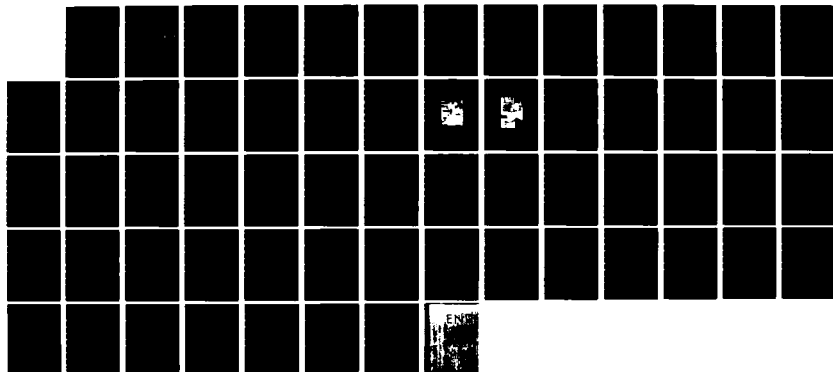
FAR INFRARED RADIOMETRIC SPECTROMETER (FIRRS)(U)  
GEORGIA INST OF TECH ATLANTA ENGINEERING EXPERIMENT  
STATION R A BOHLANDER ET AL. 29 JUL 83 GIT/EES-A-2519  
AFGL-TR-83-0137 F19628-80-C-0031 F/G 14/2.

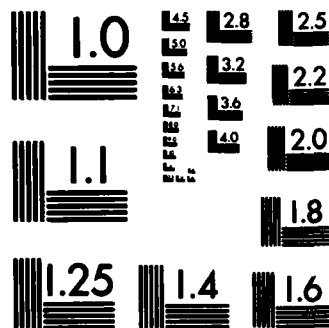
1/1

UNCLASSIFIED

F/G 14/2

NL





MICROCOPY RESOLUTION TEST CHART  
NATIONAL BUREAU OF STANDARDS-1963-A

AD-A133552

12

AFGL-TR-83-0137

FAR INFRARED RADIOMETRIC SPECTROMETER (FIRRS)

R.A. Bohlander  
D.R. Lamm  
J.W. Larsen  
M.J. Sinclair

Georgia Institute of Technology  
Engineering Experiment Station  
Atlanta, Georgia 30332

Final Report  
5 November 1979 - 30 May 1983  
29 July 1983

DTIC  
ELECTE  
OCT 14 1983  
S B

This research was partially supported by the Air Force  
In-House Laboratory Independent Research Fund

Approved for public release; distribution unlimited

DTIC FILE COPY


AIR FORCE GEOPHYSICS LABORATORY  
AIR FORCE SYSTEMS COMMAND  
UNITED STATES AIR FORCE  
HANSCOM AFB, MASSACHUSETTS 01731

83 10 12 254


This report has been reviewed by the ESD Public Affairs Office (PA) and is releasable to the National Technical Information Service (NTIS).

This technical report has been reviewed and is approved for publication.

  
JOHN H. SCHUMMERS  
Contract Manager

  
for ROBERT W. FENN, Chief  
Atmospheric Optics Branch

FOR THE COMMANDER

  
JOHN S. GARING, Director  
Optical Physics Division

Qualified requestors may obtain additional copies from the Defense Technical Information Center. All others should apply to the National Technical Information Service.

If your address has changed, or if you wish to be removed from the mailing list, or if the addressee is no longer employed by your organization, please notify AFGL/DAA, Hanscom AFB, MA 01731. This will assist us in maintaining a current mailing list.

Do not return copies of this report unless contractual obligations or notices on a specific document requires that it be returned.

UNCLASSIFIED

SECURITY CLASSIFICATION OF THIS PAGE (When Data Entered)

REPORT DOCUMENTATION PAGE		READ INSTRUCTIONS BEFORE COMPLETING FORM
1. REPORT NUMBER AFGL-TR-83-0137	2. GOVT ACCESSION NO. AD-A133552	3. RECIPIENT'S CATALOG NUMBER
4. TITLE (and Subtitle) Far Infrared Radiometric Spectrometer (FIRRS)		5. TYPE OF REPORT & PERIOD COVERED Final Report 5 Nov. 79 - 30 May 83
		6. PERFORMING ORG. REPORT NUMBER A-2519
7. AUTHOR(s) R.A. Bohlander, D.R. Lamm, J.W. Larsen and M.J. Sinclair		8. CONTRACT OR GRANT NUMBER(s) F19628-80-C-0031
9. PERFORMING ORGANIZATION NAME AND ADDRESS Georgia Institute of Technology Engineering Experiment Station Atlanta, GA 30332		10. PROGRAM ELEMENT, PROJECT, TASK AREA & WORK UNIT NUMBERS 61101F ILIROJAA
11. CONTROLLING OFFICE NAME AND ADDRESS U.S. Air Force Geophysics Laboratory Hanscom AFB, Massachusetts Monitor/John H. Schummers/OPR		12. REPORT DATE 29 July 1983
		13. NUMBER OF PAGES 60
14. MONITORING AGENCY NAME & ADDRESS (if different from Controlling Office)		15. SECURITY CLASS. (of this report) Unclassified
		15a. DECLASSIFICATION/DOWNGRADING SCHEDULE
16. DISTRIBUTION STATEMENT (of this Report)  Approved for public release; distribution unlimited		
17. DISTRIBUTION STATEMENT (of the abstract entered in Block 20, if different from Report)		
18. SUPPLEMENTARY NOTES  This research was partially supported by the Air Force In-House Laboratory Independent Research Fund		
19. KEY WORDS (Continue on reverse side if necessary and identify by block number) Millimeter                      Radiometer Submillimeter                  Spectrometer Far Infrared                    Airborne Measurements		
20. ABSTRACT (Continue on reverse side if necessary and identify by block number) The development of a sensitive and versatile Far Infrared Radiometric Spectrometer (FIRRS) instrument package is described. This system has been built by Georgia Tech for use by the Air Force Geophysics Laboratory for airborne measurements from their flying laboratory. The measurements will be of up-welling radiation in the wavelength band 0.17 to 1.7 mm. A number of advances in the state-of-the-art are described in areas such as an interferometer with high resolution and efficiency, polarizing beam dividers,		

UNCLASSIFIED

**UNCLASSIFIED**

**SECURITY CLASSIFICATION OF THIS PAGE(When Data Entered)**

narrow band interference filters and background signal reduction.

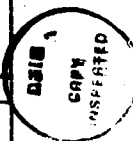
**UNCLASSIFIED**

**SECURITY CLASSIFICATION OF THIS PAGE(When Data Entered)**

# PREFACE

This report gives a summary description of a Far Infrared Radiometric Spectrometer system designed and built by the Georgia Tech Engineering Experiment Station for use by AFGL in the spectral region 0.17 to 1.7 millimeters wavelength. For detailed design descriptions, reference may be made to three other reports: a Preliminary Design Report [1], a Research and Development Design Evaluation Report [2], and a draft report [3] which serves as an operator's manual. These have been delivered to the Radiation Effects Branch of the Optical Physics Division of AFGL for their use.

Accession For	
NTIS GRA&I	<input checked="" type="checkbox"/>
DTIC TAB	<input type="checkbox"/>
Unannounced	<input type="checkbox"/>
Justification	
By	
Distribution/	
Availability Codes	
Dist	Avail and/or Special
A	



## CONTENTS

1.0	INTRODUCTION	5
2.0	BACKGROUND	7
2.1	Atmospheric Models	7
2.2	Signal Fluctuations - Clutter	12
3.0	THE FIRRS INSTRUMENT PACKAGE	16
3.1	Rapid-Scanning Interferometer	16
3.2	Telescope Subsystem	24
3.3	Detectors	25
3.4	Optical Filters	29
3.4.1	Narrow-Band Filters	31
3.4.2	Low-Pass Filters	32
3.5	Calibration Sources	33
3.6	Electronics	38
3.6.1	Head Electronics and Control Electronics	38
4.0	PROBLEMS ENCOUNTERED	46
4.1	Bearings	46
4.2	Alignment and Stress in a Double-Beam, Push-Pull Interferometer	47
4.3	Use of Two Parallel Position Encoders to Produce a Combined Position Output Signal	49
4.4	Other Problems Encountered	50
5.0	ACHIEVEMENTS	52
6.0	CONCLUSIONS	54
7.0	ACKNOWLEDGEMENTS	56
8.0	REFERENCES	57



## ILLUSTRATIONS

2.1	Theoretical transmission of the atmosphere	10
2.2	The effect of cirrus clouds and cumulus clouds on near and far infrared radiation from the sun	11
3.1	FIRRS instrument package (first view)	17
3.2	FIRRS instrument package (second view)	18
3.3	Top view of ray paths above the main instrument base plate	19
3.4	Rapid-scanning Martin-Puplett type interferometer	21
3.5	Telescope, television camera and shock absorber assembly	26
3.6	Bottom view of the detector cryostat	28
3.7	Block diagram of electronics in FIRRS	39
3.8	Servo-system functional diagram	41
3.9	Data acquisition systems functional diagram	43

## TABLES

2.1	Near-millimeter wave reflectivity of common materials	13
3.1	Narrow-band filters	33
6.1	Status of FIRRS	55

## FAR INFRARED RADIOMETRIC SPECTROMETER (FIRRS)

### 1.0 INTRODUCTION

This report describes a Far Infrared Radiometric Spectrometer (FIRRS) that will be used to survey radiation in the 0.17 to 1.7 mm wavelength band\* seen looking down from an aircraft. The instrument was built by the Engineering Experiment Station (~~ET/EES~~) of Georgia Institute of Technology for the U.S. Air Force Geophysics Laboratory, (AFGL) under contract No. F19628-80-C-0031. The instrument is intended for use on an AFGL NKC-135A aircraft.

An important initial purpose of the FIRRS will be to determine the effects of atmospheric attenuation and emission. The instrumentation will have two survey functions:

- (1) It will measure and calibrate the electromagnetic intensity spectrum received when flying over various terrain and atmospheric conditions.
- (2) Variations in the scene as the aircraft flies along will cause fluctuations in signal, often called clutter, which will also be analyzed.

It is important to determine typical levels of background radiation and its clutter to be able to assess future applications of the far infrared wavelength band.

After consideration of alternative spectrometer types, two were selected for inclusion in the FIRRS: a rapid-scanning Michelson interferometer, and a series of narrow-band interference filters. These will be used in different regimes determined by the bandwidth in temporal frequency of the clutter. Both will give high throughput efficiency. Radiation

---

\* In frequency 180 to 1800 GHz and in wavenumber 6 to 60<sup>-1</sup>.

> will be collected by a telescope with an aperture of 190 mm diameter, and will be detected by liquid helium-cooled bolometers and photoconductors.

The principal elements of FIRRS will be described in the report and the achievements made and problems encountered.

## 2.0 BACKGROUND

Increased attention is being given in the engineering community to the possible uses of radiation with wavelengths near one millimeter. Compared with microwaves, near-millimeter wavelengths offer better antenna directivity, but atmospheric attenuation becomes a serious limitation. Nevertheless, near-millimeter wave or far infrared radiation is expected to penetrate fog, clouds, smoke, etc. in many cases when visible or infrared radiation cannot do so [4]. There is a need for a better understanding of the atmospheric attenuation factor in the assessment of possible future systems. Moreover, the signatures of natural and man-made objects in the far infrared need further clarification.

Due to strong water vapor absorption, ground-based applications of the near-millimeter wavelength band will be restricted mainly to wavelengths longer than 0.75 mm and to ranges around 1 km at short wavelengths in this range [5]. There are several programs under way at Georgia Tech and elsewhere to obtain data on near-millimeter wave performance in this regime and to construct pilot systems. However, the above limitations can be relaxed for airborne operations because of reduced water vapor concentrations and other factors at high altitudes. Little has been done to measure up-welling radiation in the far infrared, and therefore a survey from an aircraft is timely, particularly for the shorter wavelengths which ground-based studies will not cover. As the wavelength becomes smaller, the power radiated by thermal sources is higher and better spatial resolution can be obtained.

Possible communications and surveillance systems are being considered by the DoD that would exploit the above-mentioned advantages of far infrared wavelength radiation (i.e., in near-millimeter or submillimeter bands).

A possible application would be to locate aircraft or rockets in flight from a satellite or aircraft platform. At shorter wavelengths strong emissions lines from excited vibrational states of water are accessible (e.g. at  $\lambda = 0.455$  and  $0.349$  mm). These are of interest in detecting the plumes of jet and rocket engines, as are numerous emission lines from other combustion chemicals that lie in the proposed range of study. This was given attention in a study [6] made by GT/EES showing the feasibility of missile plume detection in the altitude range 30 to 100 km using submillimeter wavelengths. In some parts of the spectrum, and in some atmospheric conditions, it may also be possible to monitor weather patterns, surface state, etc. Little has been done to measure up-welling radiation in the 0.17 mm to 1.7 mm wavelength band.

The wavelength range of FIRRS extends to wavelengths long enough (1.7 mm) to give the instrument some penetration to the ground. Thus, some useful comparisons with ground-based measurements will be possible. The short wavelength limit (0.17 mm) is determined by reasonable instrumental constraints (availability of detectors, tolerances in the fabrication of the interferometer, etc.) and by the onset of very intense attenuation due to water vapor.

## 2.1 Atmospheric Models

Model calculations of atmospheric transmission or emission looking down will be used here to outline the context in which the FIRRS instrument will make measurements.

Early in the research program described here, theoretical atmospheric transmission and emission calculations were made [1] which were crude in some respects but served reliably to illustrate some of the salient features and

limitations of the far infrared wavelength region. This section reviews some of the important conclusions of this effort. Molecular absorption between 0.17 and 1.7 mm wavelength is due mainly to water vapor although oxygen also contributes a few noticeable absorption lines. For simplicity, the latter are neglected here since water vapor, with its strong absorption, largely determines what can be seen in clear air.

From Figure 2.1(a), it is evident that an aircraft flying at 10 km altitude cannot see the ground except at wavelengths  $> 0.9$  mm under standard conditions. In the arctic or on mountain tops where the air can be very dry, transmission windows near 0.44 and 0.35 mm may open up. These windows can also be seen in Figure 2.1(b) where the transmission between the 10 km and 5 km levels is shown. Still shorter wavelength windows may be seen in higher altitude paths (Figure 2.1(c)).

Transmission through clouds in the far infrared is beginning to receive attention [e.g. 7]. Figure 2.2 shows measurements [8] of solar radiation as clouds pass through the field-of-view of the receiver, and compares the signals received in the near and far infrared. The one at  $1.2 \mu\text{m}$  is mainly sensitive to scattering, and the far infrared signal (0.9 to 3 mm) shows mainly the effect of absorption by clouds and associated water vapor.

The radiation up-welling to an aircraft sensor like FIRRS will comprise several components:

- (1) radiation emitted by the surface of the earth,
- (2) down-welling radiation reflected or scattered by the surface,
- (3) emission from molecules,
- (4) emission from condensed water (cloud, rain, etc.), and
- (5) scattered radiation by the same.

The molecular components in this are the most easily modeled.

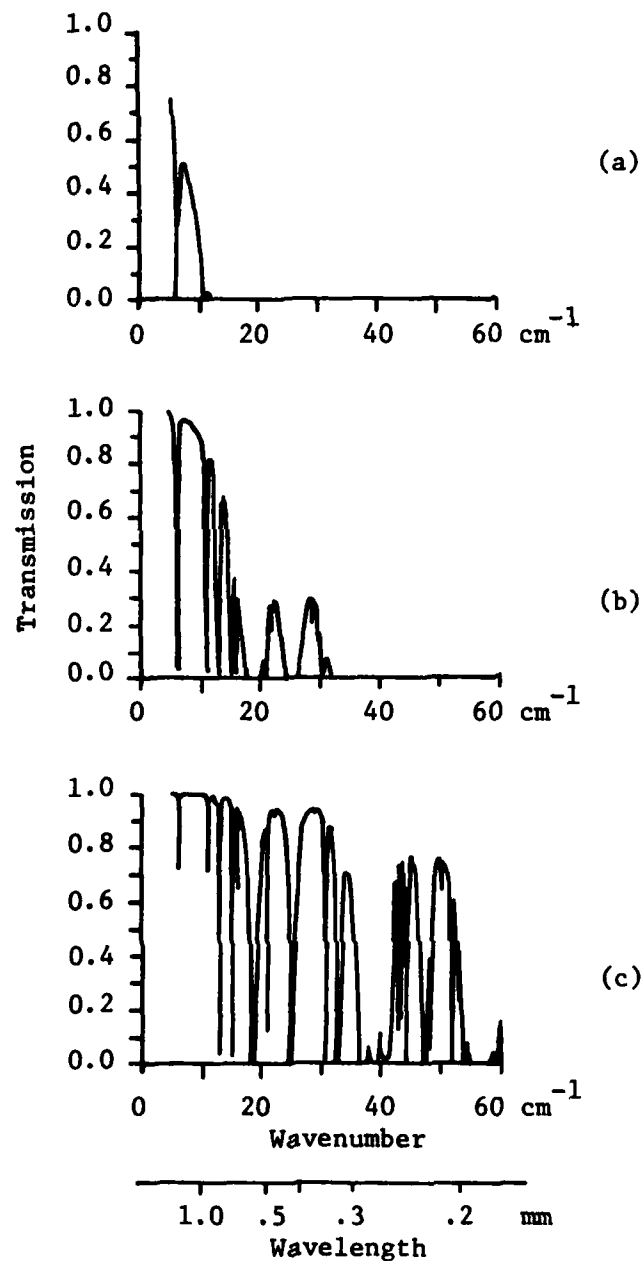


Figure 2.1. Theoretical transmission of the atmosphere between the altitudes of a) 10 km and 0 km, b) 10 km and 5 km, c) 10 km and 9 km. Water vapor density and air pressure are assumed to fall off exponentially with scale heights of 2 km and 8 km, respectively. The temperature was assumed to lapse from 293K at the surface to 230K at 10 km in a linear fashion.

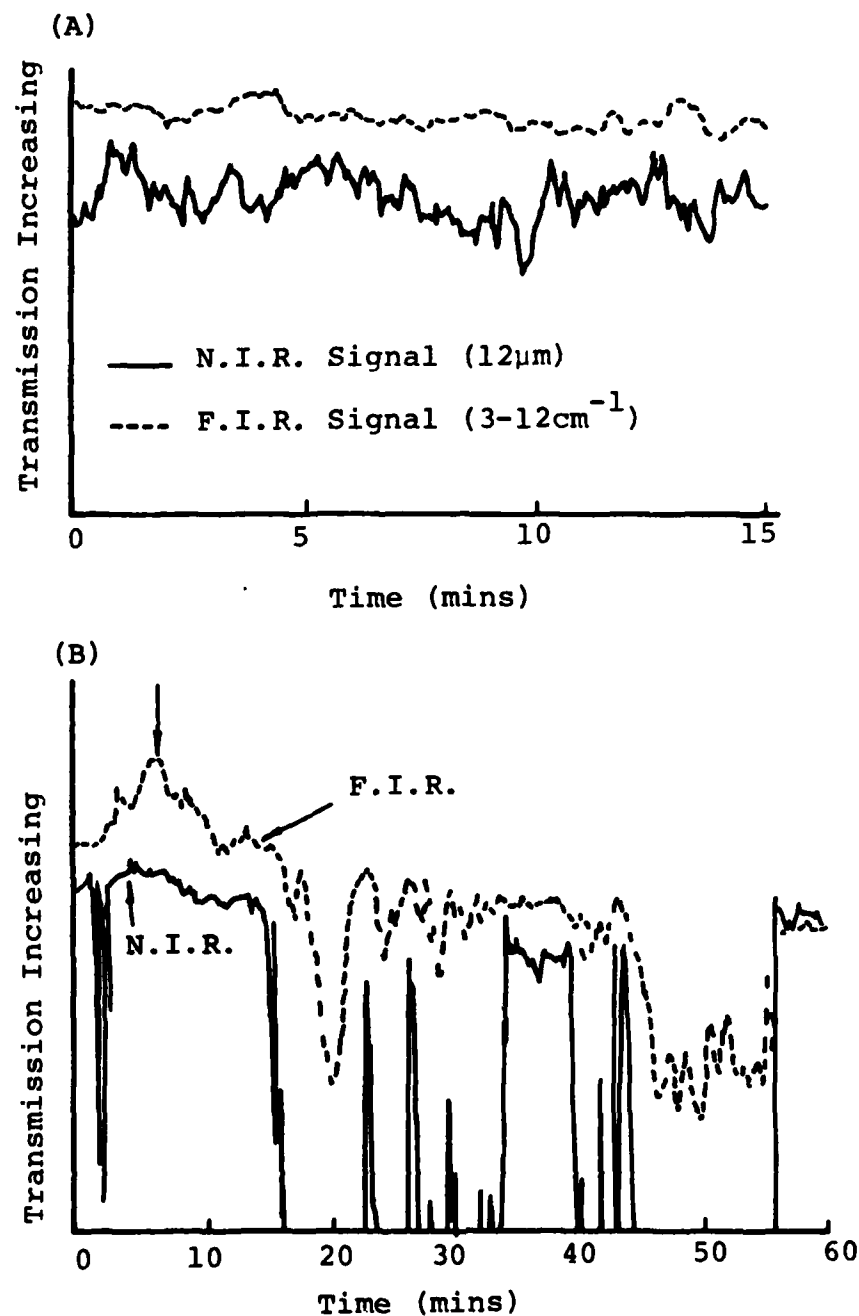


Figure 2.2. The effect of cirrus clouds (A) and cumulus clouds (B) on near and far infrared radiation from the sun. The vertical arrow in (B) indicates a change in the far infrared signal not caused by cloud. A change in the water vapor in the beam may have been responsible. (From Ref. 8)



Prediction of the contribution of condensed water is made difficult by variabilities and uncertainties in the concentrations and drop sizes in clouds and by the effects of multiple scattering. Moreover there are uncertainties concerning the parameters of ground cover. Table 2.1 lists some values of reflectivity for various natural materials measured in the laboratory. Little is known, however, about backscatter and reflection in natural settings; for example, the reflectivity of a blade of grass and the backscatter from a lawn of grass may be very different. On account of such uncertainties, a survey instrument like FIRRS has a useful role to play.

## 2.2 Signal Fluctuations - Clutter

Radiometer signal fluctuations can arise in a number of ways; for example, from

- (1) changes in molecular concentrations in the beam, especially water vapor,
- (2) changes in the terrain,
- (3) changes in clouds in the beam.

In principle, fluctuations can occur with frequencies up to approximately  $f_{\max}(z) = S/F(z)$  where  $S$  is the speed of the aircraft and  $F(z)$  is the horizontal beam width at the level  $z$  where the fluctuations are introduced. The actual upper frequency limit in the spectrum of fluctuations may be lower than the value of  $f_{\max}(z)$  if the structures causing the fluctuations are generally larger than the beam width. Since the bandwidth of the fluctuation spectrum influences the choice of a data recording scheme, the following review is given of the limited information available.

The effects of humidity heterogeneities on near-millimeter wave propagation is a topic of importance to system designers, but it is a relatively new area of study. All of the work

Table 2.1. Near-Millimeter Wave Reflectivity of Common Materials in the Wavenumber Range 5 to 60  $\text{cm}^{-1}$

<u>Materials</u>	<u>Reflectivity (%)</u>
Asphalt	5 <sup>a</sup>
Concrete	10-20 <sup>a</sup>
Grass	10-20 <sup>a</sup>
Leaves	10-20 <sup>a</sup>
Metal	20-95 <sup>a,b</sup>
Sand	2 <sup>a</sup>
Soil	2 <sup>a</sup>
Water	14-30 <sup>c,d</sup>
Wood	2 <sup>a</sup>

<sup>a</sup> Ref [17]

<sup>b</sup> depending on paint, rust, etc.

<sup>c</sup> Ref. [18]

<sup>d</sup> increases from 14% at 60  $\text{cm}^{-1}$  to 30% at 8  $\text{cm}^{-1}$

with which the authors are familiar is ground-based involving either horizontal propagation or radiometry directed toward the sky. It is also possible to draw on experience at microwave and radio frequencies, since they too are sensitive to humidity heterogeneities. From microwave astronomical observations, Hinder and Ryle [9] estimate that the most important heterogeneities in the troposphere have a horizontal scale of between 300 and 1200 m. They believe these represent the width of convective cells in the atmosphere. Recently Kemp [10] inferred a similar value for the typical horizontal scale ( $\sim 400$  m). He used intensity fluctuations in an observed signal from the sun at  $\lambda \approx 1$  mm; the corresponding fluctuation duration was 40 sec for a wind speed of 10 m/sec. It is likely that smaller scale structure exists near the ground. Preliminary measurements of sky emission at  $\lambda = 3.2$  mm have been made at GT/EES [11] which support this. Fluctuations with durations as short as 0.15 sec have been seen. Since the FIRRS horizontal beam width will be large near the ground, it will not be sensitive to fine structure like this but will be well-matched to the above estimates of convective cell sizes.

As altitude increases, it seems likely that humidity cells will increase in horizontal extent. Moreover, water vapor at high altitudes is less dense and therefore has less effect. Although the horizontal beam width of FIRRS will be small at high altitudes, it appears unlikely that humidity will cause a significant level of rapid fluctuations, approaching  $f_{\max}(z)$  for these altitudes. It is more likely that high frequency fluctuations will arise if there are thick clouds near the altitude of the aircraft. The antenna temperature looking at clouds may differ by tens of degrees from that for a clear air path to the ground. The FIRRS instrument will have a special mode of operation, described in the following section for cases when the fluctuation

frequencies may be high.

### 3.0 THE FIRRS INSTRUMENT PACKAGE

The package comprises three main assemblies. The most important of these is the measuring instrument which will be located at a downward viewing port in what was formerly the tail-boom operator's compartment in the aircraft. There will also be a vacuum pumping station near there to maintain the correct pressure in the far infrared detector. The third assembly, the controlling electronics, will be located in an existing instrument rack in the middle of the aircraft.

Figures 3.1 and 3.2 serve to give an over-all picture of the measuring instrument. The spectrometer and detector units are located above the supporting tube which houses a telescope that collects the radiation to be measured. The supporting tube attaches to a gimbaled port in the aircraft which permits limited pointing of the telescope. The gimbal assembly, known as the "large eyeball", has been made by AFGL, and for the purpose of this report is considered to be part of the aircraft. On the side of the supporting tube, a bore-sighted television camera is shown which will document the visual scene corresponding to the direction measured by the far infrared instrumentation. The following sections will describe the various modules of the instrumentation.

#### 3.1 Rapid-Scanning Interferometer

There are actually two types of spectrometer in FIRRS which can be used interchangeably: a rapid-scanning interferometer and a set of narrow-band interference filters. This section will deal with the former. The interferometer is of the Martin-Puplett type which incorporates polarizing beam dividers. The principles of operation for this type of interferometer were covered in [1]. As a brief review, radiation from the telescope is polarized and reflected into the interferometer by beam divider BD1 shown in Figure 3.3.



Figure 3.1 FIRRS instrument package - view from the side which will be on the left side of the aircraft.



Figure 3.2 FIRRS instrument package - view from the side which will be toward the front of the aircraft.

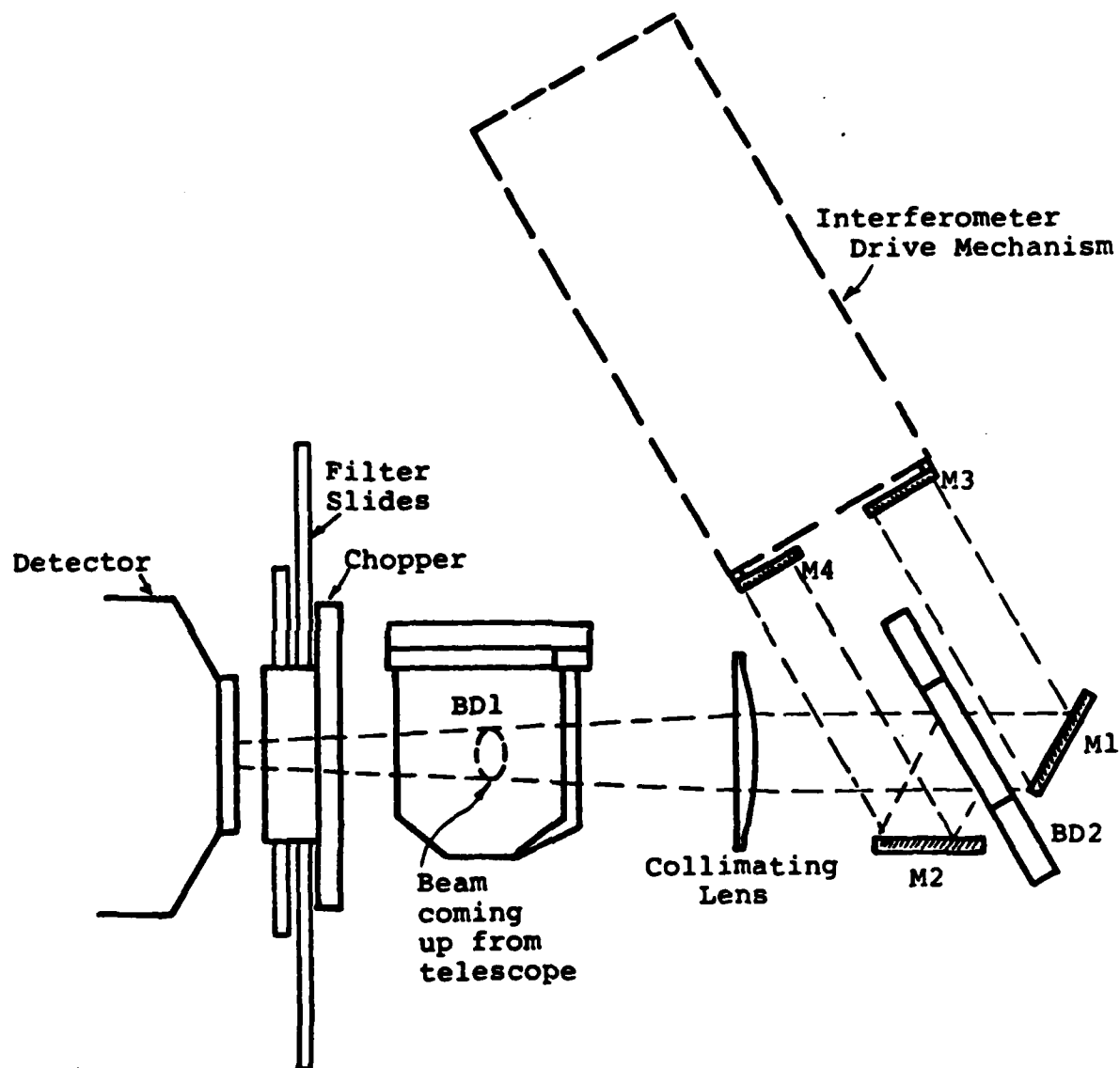


Figure 3.3. Top view of ray paths above the main instrument base plate. Mirrors, M. Beam dividers, BD.



It is then split at BD2, reflected by mirrors M1 and M2, and returned by the scanning mirrors M3 and M4. These act to change the difference in path length followed by the two beams in the interferometer. Interference between the recombined beams acts to modulate the state of polarization, and radiation with the correct polarization is directed through BD1 toward the detector unit. The Martin-Puplett type interferometer [12] is gaining recognition for having high efficiency over wide wavelength bands. The optical layout used in FIRRS is similar to ones described in the literature except as regards the mechanism of scanning. Some of its features are adapted from a rapid scanning mechanism which has been developed at AFGL [13].

It is necessary for the scanning mirrors in the interferometer to move in such a way that the plane of each reflecting surface is always parallel to the initial plane. In Figure 3.4 two levers  $\ell_1$  and  $\ell_2$  are shown which pivot on a base. The ends of these levers connect through pivots to mirror carriers. The angle of the lever  $\ell_2$  can be changed by the torque motor whose armature is attached to the lever and whose field is attached to the base. Lever  $\ell_1$  follows the angle of  $\ell_2$ , and the mirror carriers and levers form a parallelogram. Thus, in principle, plane parallel motion of the mirrors attached to the carriers is achieved.

Though similar to a scanning mechanism used by AFGL [13], the GT/EES design differs in several respects which permit higher spectral resolution to be achieved. In the AFGL design, only one mirror is translated by levers on one side of the base, and the mirror has a shorter range of travel. This limitation arises in the lever pivots used by AFGL which are of a torsional type whose deflection must be constrained to prevent strain failure. The pivots used in the GT/EES design are based on jeweled bearings and the angular deflections permitted,  $\pm 25^\circ$ , are about five times that allowed by the particular torsional pivots used by AFGL. Since spectral

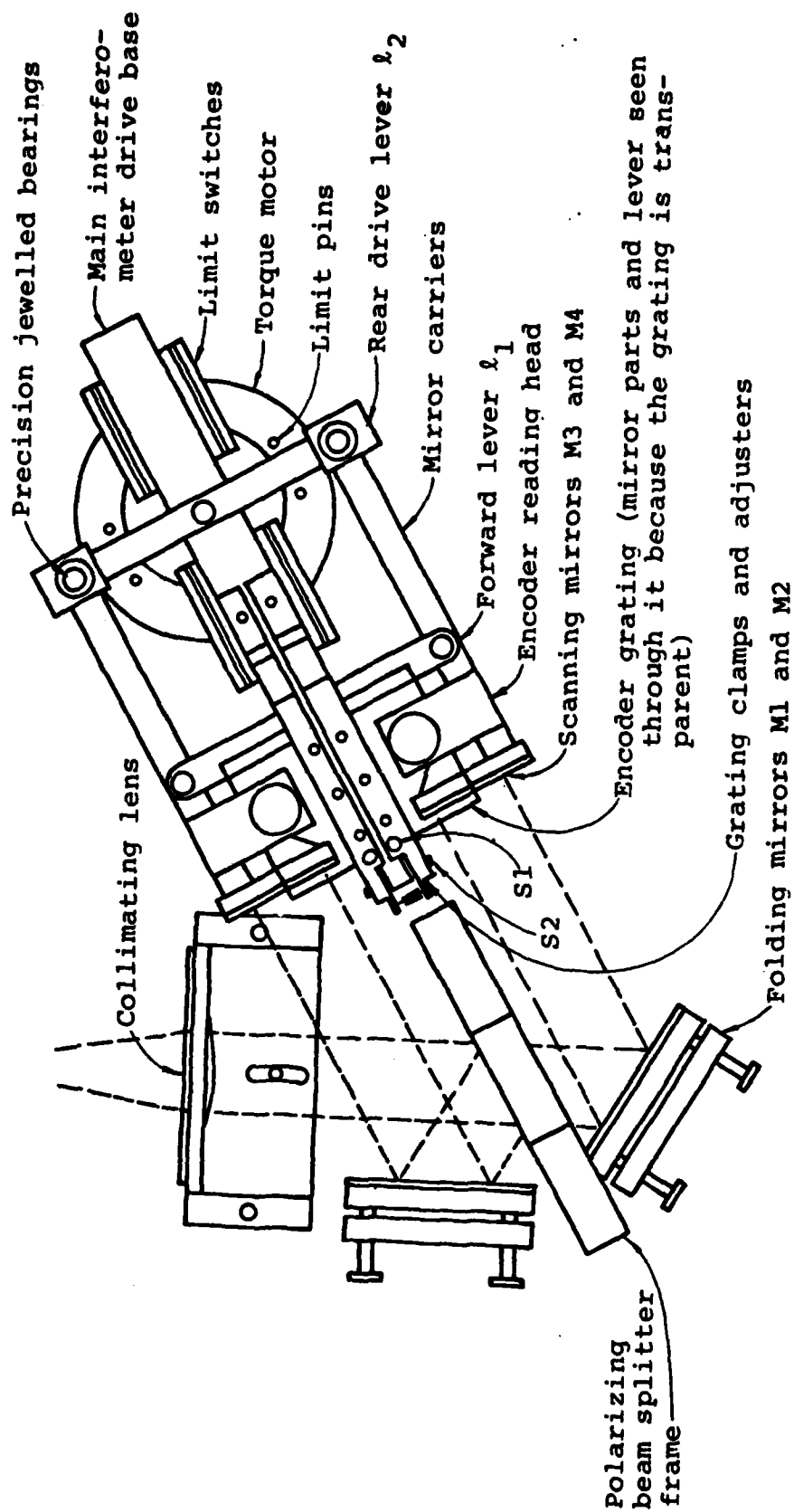


Figure 3.4. Rapid-scanning Martin-Puplett type interferometer made at GT/EES. Wiring omitted for clarity. Dashed lines illustrate ray paths. Grating elevation adjusting screw S1. Grating azimuth adjusting screw S2.

resolution depends on the range of path differences introduced by the scanning mechanism, higher spectral resolution is achieved in the FIRRS by moving the mirrors farther. The maximum path difference and spectral resolution is further increased by a factor of two because one mirror in each interferometer beam is moved, one in opposition to the other. An additional benefit of this design is that the masses on each side of the levers are well-balanced.

There are two types of polarizing beam dividers used for millimeter and submillimeter wave applications, and both have been provided for use with the FIRRS. One type is available commercially and is made by wrapping thin wires tightly around a frame and binding them by an adhesive or by metal plating. The spacing must be small compared with wavelengths of interest, and the elements ordered from SPECAC have a grating period of  $12.5\text{ }\mu\text{m}$  and wires of diameter  $5\text{ }\mu\text{m}$ . However, it is difficult to hold a tolerance on this spacing and inspection under a microscope has revealed that individual wire pairs are quite randomly spaced with a significant fraction of the wires touching each other. Another general problem area is ruggedness. Those wire gratings that are held by adhesives have been reported in private communications to have problems with susceptibility to fatigue when subjected to temperature cycling and vibration. For this reason the type ordered for this program were ones bonded by plating, but there is no data on their actual resistance to these mechanisms. However, in any case, such beam dividers are extremely fragile; the slightest accidental poke can ruin a costly element.

A preferred alternative has been successfully fabricated at Georgia Tech. In these an aluminum coated thin Mylar film substrate ( $6.4\text{ }\mu\text{m}$  thick) is etched to give metal strips of width  $4\text{ }\mu\text{m}$  and a grating period  $10\text{ }\mu\text{m}$ . The accuracy of

such a grid is excellent and the substrate gives added strength and ruggedness. If sagging of the stretched film should occur, it can readily be restretched. At the beginning of the program, it was not known for certain that this type of beam splitter would, however, perform as well in terms of the degree of polarization and transmission as the best of the wire grid polarizers. A theoretical study suggested it was feasible, but early tests of sample polarizers prepared in another laboratory showed a discrepancy with the theory. By comparison with theory, observed transmission decreased faster with decreasing wavelength (for the plane of polarization perpendicular to the grid strips). At long wavelengths by comparison with the grid period, however, the transmission is controlled primarily by the optical properties of the substrate, and here agreement with theory is good. Therefore, the problem noted above could be avoided by making grids with very fine strip spacings. This plan was implemented although the required tolerances proved quite demanding. An unexpected difficulty was that gases evolved in exposing the photoresist to ultraviolet radiation and tended to lift the film away from the master enough to ruin the pattern. This was overcome by backing the film with the flat aluminum disc, and then applying sufficient pressure to keep any evolved gas films thin. The beam splitters which have been fabricated appear to have excellent uniformity in the etched pattern.

Optical performance tests for the final product have been performed, and transmission and rejection of the appropriate polarizations is seen to be excellent over the frequency range of the FIRRS. The transmission at the highest frequency in the FIRRS range is only down to 92%; although this is believed adequate, it could be improved in principle with the same technique by the use of still thinner Mylar which is commercially available.

### 3.2 Telescope Subsystem

The telescope is a Cassegrain design with spherical mirrors. The two principle design constraints are (1) that the primary mirror diameter (190 mm) be as large as permitted by the aperture of the "eyeball" gimbal, and (2) that the effective focal ratio (7.8) be consistent with the desired angular resolution (of the scene below the aircraft) and frequency resolution at the maximum wavenumber to be measured by the FIRRS. The actual focal lengths have been lengthened somewhat since the preliminary design to allow more room for necessary fittings between components, but the above constraints remained fixed.

Since the focal ratios used were not too small, spherical optics could be used throughout at a considerable savings in cost over aspheric surfaces. A ray tracing study was conducted (1) to show the location of the minimum blur circle of the telescope that results from spherical aberration, (2) to establish the correct location of the collimation lens which is also subject to spherical aberration, and (3) to confirm that the sizes of the secondary mirror, collimating lens (for the interferometer), and the interferometer mirrors had been correctly chosen.

The telescope interfaces to the AFGL eyeball gimbal via the "telescope support tube". The connection is not completely rigid, however, in the interest of reducing the transmission of shock and vibration to the telescope and thence to the interferometer and detector. There are three potential problems which shock and vibration isolation should attempt to prevent:

- a) damage to somewhat fragile detector and interferometer components
- b) dynamic distortion of the alignment of the interferometer

c) microphonic noise input to the detector.

The need to seal the telescope to the "telescope support tube" considerably complicates the shock mounting design in that this prevents the straightforward use of any commercially available, standard shock mounts in this interface. The solution that has been attempted makes the whole telescope barrel and "telescope support tube" into a shock mount as shown in Figure 3.5. The "intermediate tube gaskets" (made of silicone rubber) act like piston rings and serve to center the barrel in the outer support tube. The "silicone rubber gasket rings" shown serve to give cushioning against axial motion and make the pressure seal. The filler shown between the two intermediate tube gaskets" is at present cork, the thickness of which is carefully established so that the filler rubs on both the telescope barrel and the telescope support tube. This is intended to act as a deadener to vibration transmitted up the support tube. In addition, commercial shock mounts are located on the upper plate of the "telescope tube". These were selected as suitable for all purpose aviation use and on the basis of a match in the load range.

### 3.3 Detectors

The two most commonly used detectors in the wavelength range of the FIRRS are the Germanium bolometer, which covers the entire range, and the InSb photoconductive detector, which covers the range only from about 0.3 mm wavelength to longer wavelengths. The former, while more sensitive and wider in its wavelength coverage, is also slower. With a response time which is usually not shorter than 5 msec, such detectors are not suitable for use with rapid scanning interferometers. FIRRS, for example, requires sampling at an interval at least as small as 0.4 msec for the shortest wavelength (0.17 mm) and for the scanning speed (mirror speed, 5 cm/sec) for which it

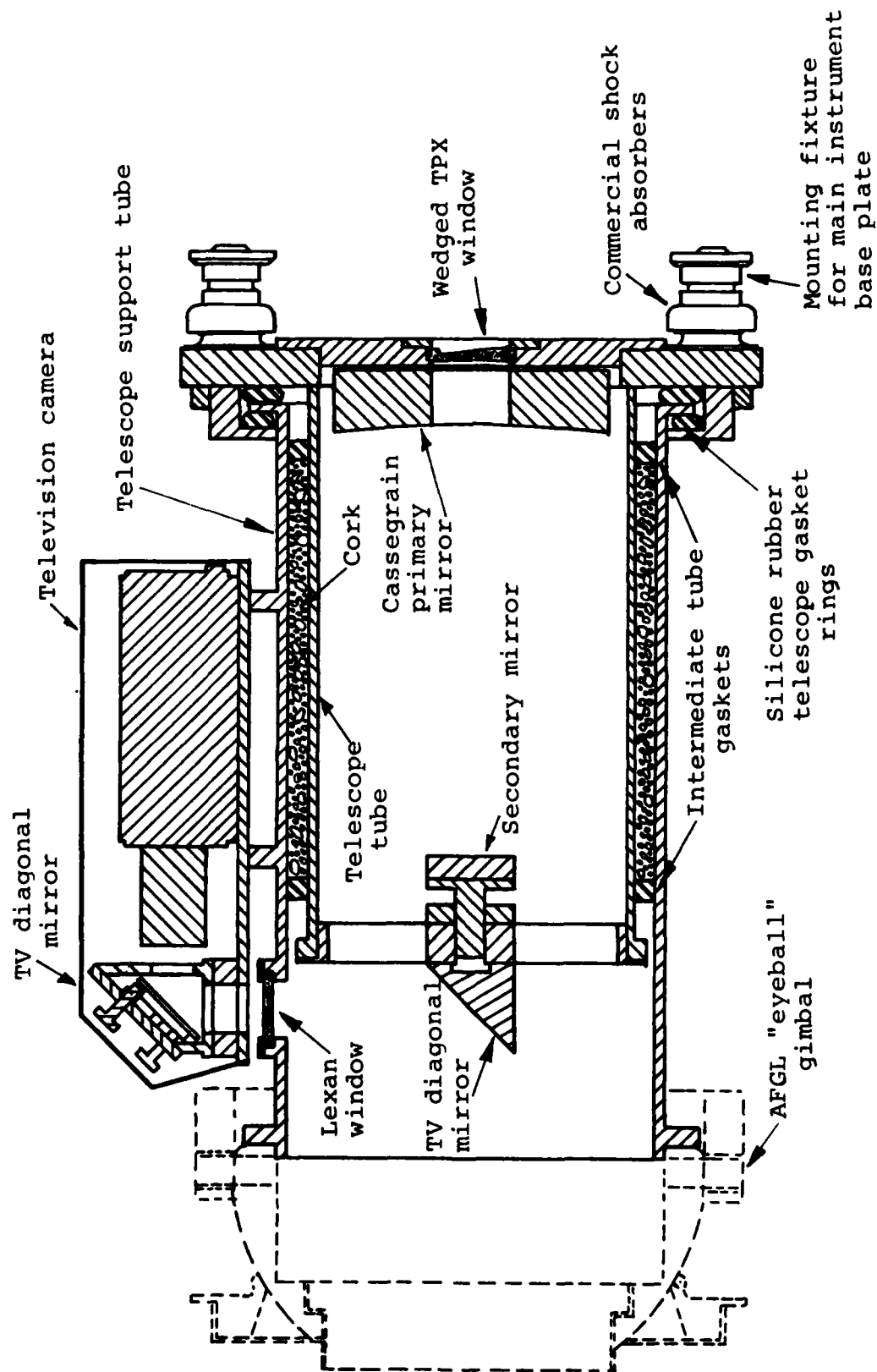


Figure 3.5. Telescope, television camera and shock absorber assembly

was designed. On the other hand, an InSb detector of the hot electron type is frequently used as a mixer element with IF frequencies in the MHz range, so these are quite fast enough for rapid scanning interferometry (with the element used not as a heterodyne detector, but as simply a direct optical power sensing element). In exchange for this speed, one gives up an order of magnitude in sensitivity and leaves the part of the FIRRS' wavelength range 0.3 to 0.17 mm uncovered. GaAs photoconductive detectors for this range have been made but are unavailable commercially. Fabrication of such detectors was not within the scope of the contract reported on here. All of these matters were discussed in considerably more detail previously [1] and no change of substance has occurred.

The detector system provided with the FIRRS comprises both types of detector element mounted in a liquid helium coolable cryostat, Model HD-3 (8) (L) made by Infrared Laboratories, Inc. A sketch is shown in Figure 3.6 of the layout of a bottom view of the cryostat with the bottom lids cut away. It may be seen that each detector is mounted in a cavity into which radiation enters by a coupling cone of a particular design known as a Winston cone [19]. Prior to this, a cooled optical low-pass filter intercepts the beam and strips off the high frequency radiation which would otherwise cause unwanted interferometric aliasing of signals and could increase detector noise. Radiation enters the cryostat via low-loss, wedged TPX windows. The purpose served by the InSb element is to record signals when the rapid scanning interferometer is used, as discussed above. The Germanium bolometer is to be used with narrow-band filters when the interferometer is adjusted to a path difference where the signal is high and locked there, as discussed in the following section. In this mode, high sensitivity at



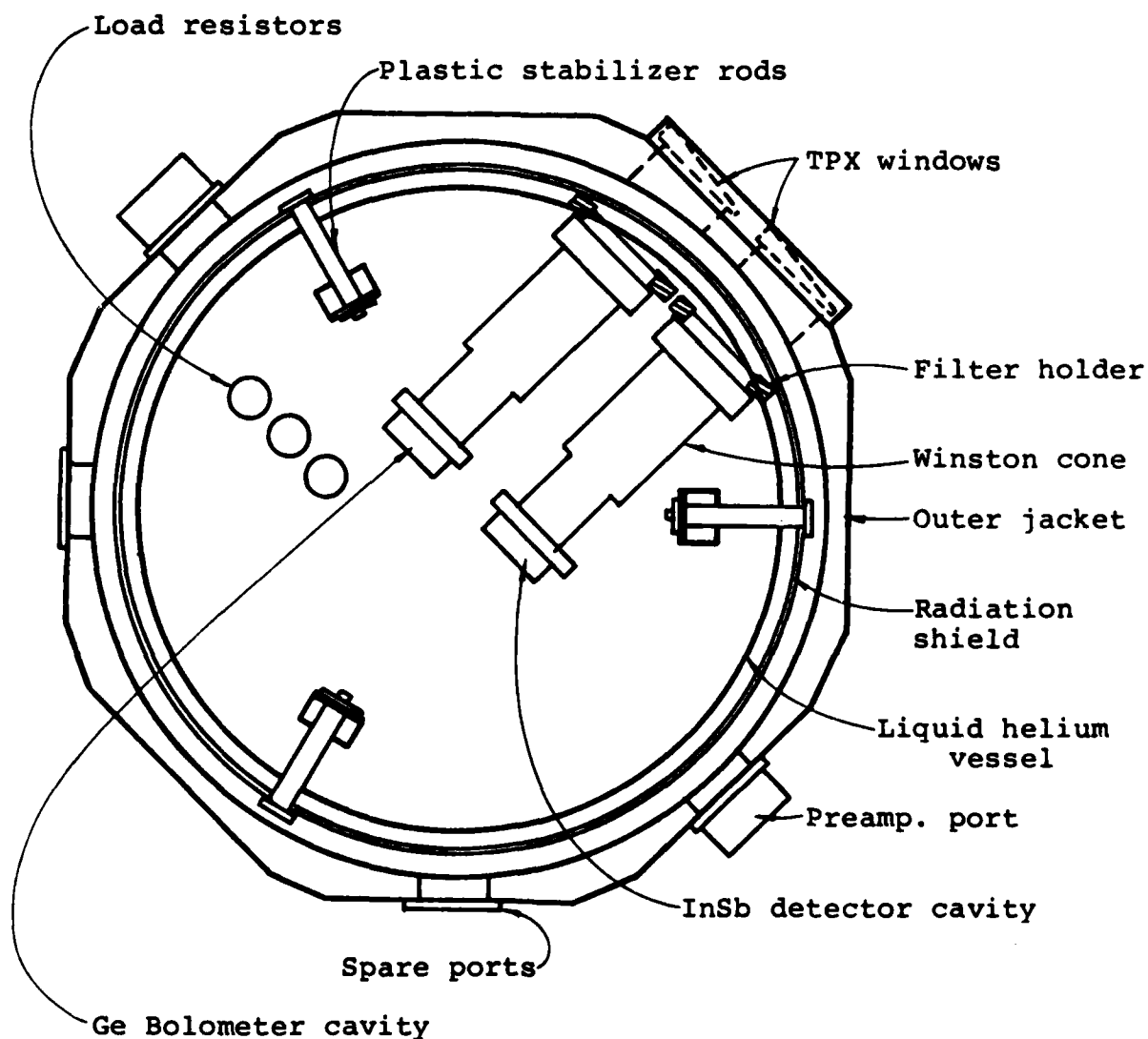


Figure 3.6. Bottom view of the detector cryostat with the bottom covers removed. The dimensions of the Winston cones [19] determine the overall field of view of the system to be in the range 22 to 12 mrad, respectively, for wavenumbers in the range 6 to 60  $\text{cm}^{-1}$ .

selected frequencies is the objective.

An additional plate has been added to the bottom of the cryostat to facilitate selecting one or the other detector element for use. This plate is grooved and can be manually slid on nylon tracks on the "main instrument base plate". In this manner, the detector can be translated to align the optical axis of either detector with the optical axis of the collimating lens associated with the interferometer. When the required position is reached, the detector baseplate is locked down with four thumb nuts and the bolts which are set into the "main instrument baseplate".

When the Germanium bolometer is used, significantly increased sensitivity can be achieved by reducing the vapor pressure over the liquid helium in the cryostat. Some improvement, perhaps a factor of two, can also be obtained for the InSb detector. This reduction in pressure is achieved by attaching a vacuum line from a high throughput vacuum pump to the detector.

### 3.4 Optical Filters

There are two principal purposes served by the optical filters provided with the FIRRS. First, low-pass filters must be used to provide a high frequency cut off of radiation to the detectors, to reduce detector noise and to avoid the well-known problem of aliased signals that occur in Fourier spectroscopy unless adequate filtering is provided. Second, as discussed in [1], it was desirable to provide in the FIRRS an alternate to Fourier spectroscopy for use in special cases where time resolution of far infrared signals was of such importance that the resolution of multiple frequencies in the far infrared spectrum could be sacrificed. The alternative proposal was the use of narrow-band interference filters. Both narrow-band and low-pass

filters will be discussed in following sections.

To facilitate the use of the narrow-band filter option, it was desirable that a rapid changeover be possible from the use of the interferometer, for instance when during a flight one starts to fly over nearby clouds, in which case the temporal modulation rate may suddenly increase. It was found to be impractical merely to switch the interferometer out of the beam, by interposing mirrors for example, because (1) the interferometer's collimating lens is also the lens which condenses radiation on the detector input, (2) the path length through the interferometer is chosen carefully for good beam containment and this would be upset by a shorter path, and (3) polarization rotating mirrors would have to be used or beam divider BD1 replaced with a mirror. In short, simplicity is served by leaving the interferometer in the optical system when the narrow-band filters are in use. All that is required is for the interferometer to be locked at a fixed setting of path difference for which the signal level is high, and this is achievable with the servo-controlled interferometer drive which is under microprocessor control.

A compact filter assembly has been devised to hold the narrow-band filters and a number of related components. The filters themselves are mounted in a long nylon holder with multiple apertures that can be slid through a mounting block fixed to the interferometer plate. An aperture in the block provides an opening for the optical path between the collimating lens and the detector. The filter slide lines up one or another filter with this aperture with the aid of a sprung ball and detents. The filter slide is moved with the aid of a handle which protrudes through the top of the interferometer case. This same block also holds a smaller slide that carries low-pass filters that must be

used in conjunction with the narrow-band filters. It operates in the same manner. The narrow-band filter slide has room for four filters and one blank, while the low-pass filter slide has room for two and one blank. The aperture of the filters is 25 mm and is large enough that vignetting is not a problem.

The low-pass filters mentioned above are intended to defeat harmonic, high-frequency leaks in the narrow-band filters. The primary low-pass filters introduced at the beginning of this section are a separate set which are mounted inside the detector. These are at the temperature of the cryogens in the detector so that they not only block high frequency radiation that comes from the interferometer, etc., but also emit negligible background radiation. Both functional types of low-pass filter will be discussed.

Finally, the filter block also includes a chopper assembly. The purpose of the chopper is to provide modulation of the signal when the filters are in use. When, instead, the interferometer is in use, the filter slides are moved to the blank position and the chopper stopped with the blades open.

#### 3.4.1 Narrow-Band Filters

Interference filters of two types can be used to make narrow-band filters for far infrared wavelengths. Background information is given in [1] and previous theoretical and experimental work is described in references [14] and [15]. The latter two were written by Dr. G.D. Holah who has fabricated the interference filters for the FIRRS, with the assistance of Mr. J.H. Rainwater who conducted the spectral measurements. One of the two types of filter is the simple Fabry-Perot type which consists of two metal meshes which have fairly high reflectivity at the wavelength

of interest and which have their planes parallel and spaced apart by half a wavelength. The second type incorporates three meshes, each spaced half of a wavelength from the next. Previous discussions [15] indicated that the second type, the so-called double-half-wave (DHW) filter, was superior to the first in having greater rejection away from band center and better transmission near band center.

It was realized after work began that it was impractical to implement a DHW design for these specifications since one cannot set the wavelength at will. The spacing of the meshes is by shim rings [14,15], and firstly not every possible shim thickness is available, and secondly the degree of compression used in assembly makes the final thickness somewhat unpredictable. Therefore, it was decided to make Fabry-Perot filters. In the work done at Georgia Tech, great care was taken in maintaining the parallelism between the meshes during fabrication. As a result, Fabry-Perot filters have been made with higher in-band transmissions than ever before for comparable bandwidths. They are in fact as good in this respect as DHW filters and in better agreement with theoretical performance than previously achieved. Table 3.1 is included which compiles the present results. The column labeled minimum transmission refers to the transmission a few reciprocal centimeters in wavenumber away from band center and is the maximum value theoretically possible given the peak transmission and the width of the filter passband. The column marked estimated passband width is derived by estimating the deconvolution of the observable width and the spectral resolution used in the measurements. All of the design specifications have been met for the filters which have been made. The one centered at  $50.5 \text{ cm}^{-1}$  has not been made, as difficulties were encountered with the test equipment available. In particular, to make a Fabry-

Table 3.1. Narrow-Band Filters made at Georgia Tech - Centered at Wavenumbers Shown

Wavenumber $\text{cm}^{-1}$	Transmission %	Minimum Transmission %	Bandwidth (Full width at half maximum) $\text{cm}^{-1}$	Mesh* Wire Period microns
9	84	0.9	0.6	254
10.9	88	0.24	0.35	203 & 169
22.5	71	0.39	1.1	102 & 91

\* For reference: This is the difference between wires in the planes of the meshes used.

Perot type filter here one needs an evacuable Fourier spectrometer to measure the filter's spectral characteristics during fabrication, and one with an evacuable chamber in which the Fabry-Perot jig can be placed and operated remotely. Such facilities, while soon to be available at Georgia Tech, were not so during the contract period and could not be addressed.

#### 3.4.2 Low-Pass Filters

Interference filters were also planned both for detector filters and for the reinforcement needed in blocking the high frequency leaks mentioned above. Up to ninety-five percent transmission in the pass region has previously been achieved [14] as well as reasonably sharp edges and good high frequency rejection. However, difficulties were encountered with the fabrication of these which have prevented their completion. The type of mesh used in narrow band filters (above) are conventional wire meshes, also called "inductive meshes" [14], and are available commercially from an electroforming process. Those used in low-pass filters are the negative images of conventional wire meshes [14] and are termed "capacitive meshes". Whereas "inductive meshes" consist of free-standing wires, capacitive ones consist of thin metal plates on a thin plastic film substrate.

The designs attempted at Georgia Tech were similar to previous ones implemented elsewhere [14] and incorporated four meshes separated by spacers with appropriate thicknesses. The necessary metal patterns were made by evaporating aluminum through inductive meshes such that the latter shadowed the Mylar film substrate. Apparently the control of the metal thickness and sharpness with this technique was not adequate to obtain the expected spectral characteristic

of such meshes as tested individually. What was found was that both the individual meshes and the stacks of meshes cut off at much lower wavenumbers than intended. In previous work [14], successful filters were made by a photolithographic process, but such tooling was not available during the course of the project. Given pressures on the available project resources from other areas of the project, work on the low-pass filters had to be put in abeyance and has not been completed.

It was most important, however, that the detector not be left without low-pass filters. Those filters which Infrared Laboratories provided for mounting on the radiation shield were left in place; namely, black polythylene and quartz. Moreover, the filter for the Germanium bolometer provided by the manufacturer was reinstalled in the filter receptacle after refurbishing. This is a Z-cut quartz plate coated with garnet powder and a CsI element in series, and the garnet powder was replaced by Georgia Tech after it was damaged. Data on the original filter from the manufacturer shows good performance, but there has not been an opportunity to repeat the measurement since the refurbishing at Georgia Tech. The low-pass filter for the InSb detector is a standard combination of crystal quartz and black polyethylene. This is mainly required to block conventional near infrared radiation since the hot electron effect in the far infrared cuts off at 30 to 50  $\text{cm}^{-1}$ .

### 3.5 Calibration Sources

Calibration sources have been constructed in a form similar to that used in the infrared by AFGL. They are built for use in the aircraft, and since the telescope is sealed in flight, they cannot be inserted in front of the telescope. Instead, they are designed to fit a receptacle at the



intermediate focus of the telescope, and to calibrate the instrument between that spot and the detector.

Each source consists of a thermal emitting unit set in a bed of insulation and an outer metal skin which has a handle attached. One is fitted with resistor heaters which are powered from the receptacle and controlled in temperature by a commercial controller in the interferometer enclosure. Temperature sensing for control is via an RTD set deep inside the emitting unit; in addition, a thermistor is also buried inside for connection to the temperature monitoring unit. Only a few minutes warm-up time is required, and stability to  $\pm 0.1^{\circ}\text{C}$  may be expected. The other calibration source is made to be dipped in liquid nitrogen and the handle is thus constructed of an insulating plastic which can also act as a hanger for suspending the source in the bath. The cold source does not have resistive heaters, but the insulation around the back of the emitting unit is channeled and the outer skin perforated to permit liquid nitrogen to percolate through when it is in the bath. This source has a thermistor like that in the hot source so that its temperature can be monitored when it is placed in the receptacle.

The emitting units are a composite of a metal backing and a molded front surface. The molded compound is an epoxy loaded with absorbing ferrite particles, manufactured by Emerson and Cumings as compound CR-117. Since the dielectric constant of this material is high, it is not only a good absorber, it is also naturally a good reflector for normal incidence. The latter is not desirable in a source of thermal radiation, and to avoid this problem, it is desirable [16] to arrange that the incidence angle be the Brewster's angle, for at this angle reflection is a minimum.

Prior to the work in this contract, the dielectric-properties of these compounds were not known for the wavelength range of the FIRRS. The manufacturer had published data only in the microwave region, and some data were available from Georgia Tech at wavenumbers as high as about  $6\text{ cm}^{-1}$ . At this wavenumber, minimum reflection occurs at an incidence angle of around  $77.4^\circ$ . During the present contract, measurements were conducted with a submillimeter laser to determine the angle of minimum reflection over a wide wavelength range. It was found that the minimum reflection angle did not vary much with wavelength.

The emitting/absorbing units use the above principle and remain compact by virtue of being molded in a series of triangular ridges with an apex angle of  $25.2^\circ$ . This angle was convenient as one for which there was existing tooling, but it was also close to optimum. The residual reflectance may be estimated to be at least as low as 0.01, since at least two reflections must occur. For the radiation to experience the Brewster effect, its polarization must be plane polarized perpendicular to the ridge lines of the emitting/absorbing unit. The relevant polarization is that for maximum reflection by beam divider BD1. Thus, as seen from above, the ridge lines of the source and the metal strips of the polarizer must be orthogonal. The metal backing of the emitting/absorbing units is designed to enhance thermal conduction and thus thermal uniformity.

### 3.6 Electronics

The electronics subassemblies prepared for FIRRS comprise a number of chassis and modules as diagrammed in Figure 3.7. Part of the units are designed to be used near the spectrometers and telescope in the tail of the aircraft, but to be consistent with normal operating procedures, most of the electronics equipment will be located in the center of the aircraft where most electronic consoles are located. Electrical interconnection between the two areas is accomplished with a multiplexed data bus, coaxial analog signal cables, and power supply lines. Of the units shown, Georgia Tech has built the Head Electronics, Control Electronics, Remote Keyboard, Calibration Source and Pump Station. Summaries of the two key modules, the Head Electronics and Control Electronics follow. Reference may be made to [2] for details concerning any of the electronics.

#### 3.6.1 Head Electronics and Control Electronics

These key modules have several functions:

- 1) Servo-control of the interferometer
- 2) Data acquisition (far infrared signals and auxiliary information such as run times and instrument temperatures)
- 3) Formatting data for recording
- 4) Data display
- 5) Overall control of instrument operation

The two models will not be discussed entirely separately since responsibility for most of these functions is shared between the two.

Two microprocessors are contained in the Control Electronics to coordinate and implement many of these functions. One of these, termed the control processor, is responsible for all of the high speed spectroscopic activities; namely servo-

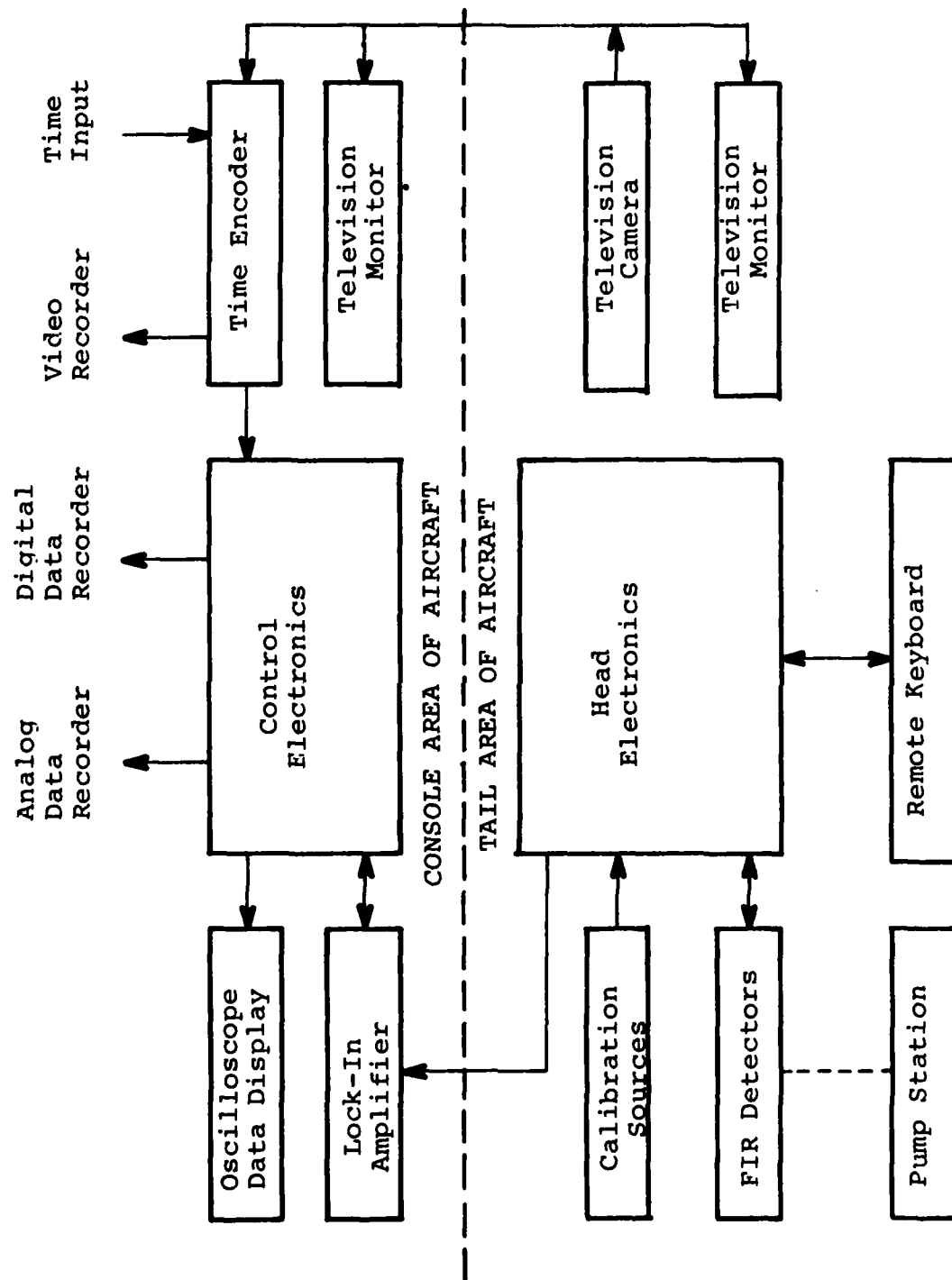


Figure 3.7. Block Diagram of Electronics in FIRRS

control of the torque motor driving the interferometer and analog to digital conversion of far infrared signals. The other microprocessor, termed the display processor, is responsible for interpreting all keyboard inputs from the operator and for all status and data display functions.

The Head Electronics contains primarily analog circuitry and interfaces between digital and analog circuits. Used in combination with the microprocessors in the Control Electronics, these circuits implement a hybrid (analog/digital) servo-system for the control of the movable mirrors in the interferometer. This servo-system positions the mirrors in one of two modes as determined by the commands it receives via the multiplexed data transmission lines from the control processor. The mirrors are either held in a given position or driven at a constant velocity (the two modes of operation) by a full rotation brushless DC torque motor. The servo-loop control circuitry supplies a control voltage to a power servo-amplifier used as a voltage controlled current source (VCC) which supplies current to the torque motor. The mirror position is determined by a pair of modular incremental position encoders, whose conditioning electronics closes the feedback loop by supplying information to the position counter. The position counter supplies position information to the servo-loop control circuitry and to the control processor. See Figure 3.8 for a functional block diagram of the servo-system.

There are two major subsystems which comprise the data acquisition system. These are the far infrared data signal processing system and the data sampling systems (which is used to determine when the data is sampled). The first of these systems takes an analog signal from a detector and produces both an amplified analog and a digital signal which can each be recorded on existing AFGL recorders. The second

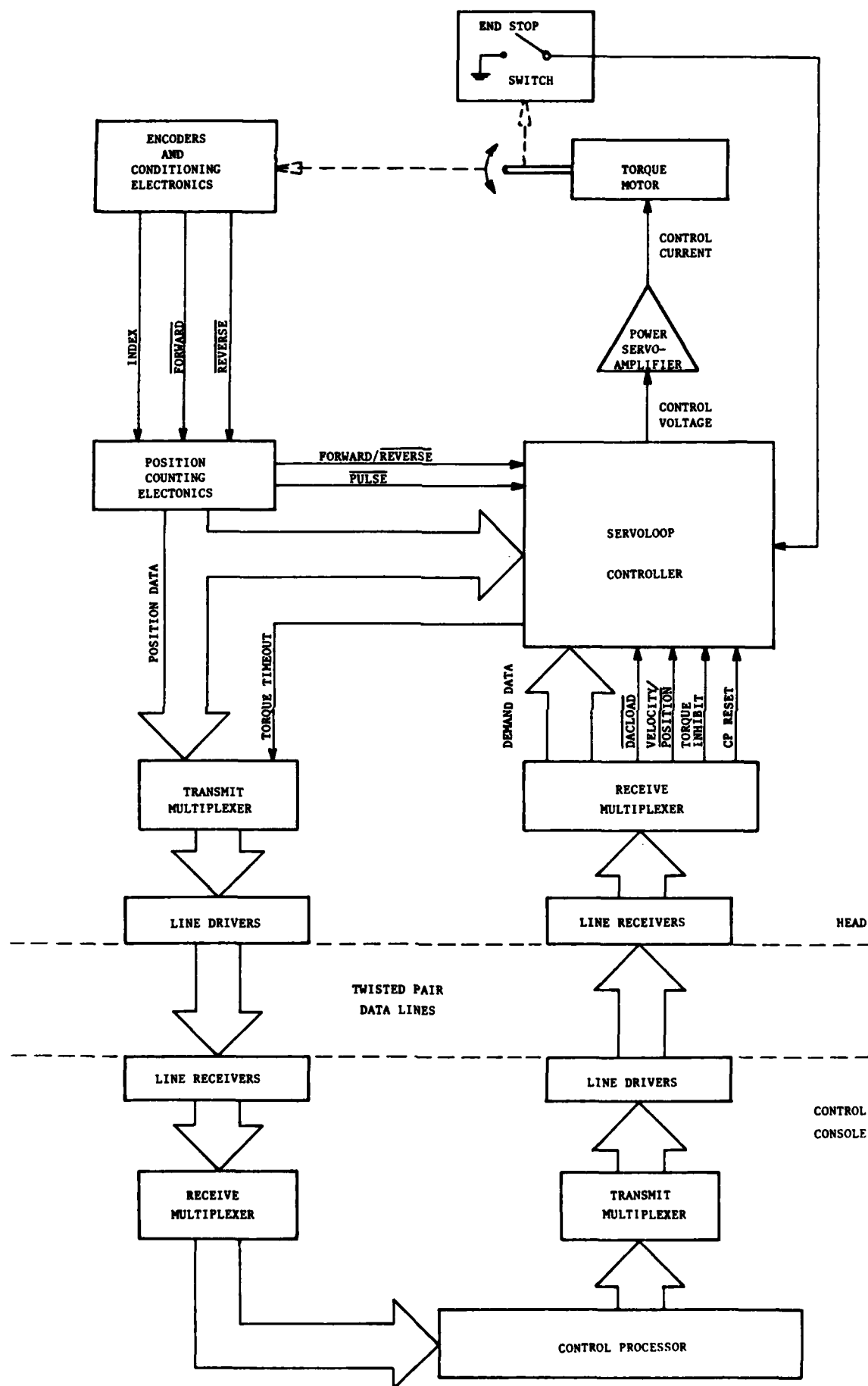


Figure 3.8. Servo-system functional diagram

subsystem is used to monitor and record changes in the path length difference in the interferometer and to determine the digital sampling rates for the first subsystem. A functional block diagram is shown in Figure 3.9.

The far infrared data signal processing system is responsible for the monitoring and recording of the far infrared power level passing through the FIRRS. Two independent cooled semiconductor detectors are used to convert the FIR radiation to a voltage signal. Each detector is associated with its own integral preamp described in the manufacturer's literature. The analog signal from one of the detectors is switched into the downline circuitry using the detector select switch which is controlled by the control processor. The signal is then amplified by a programmable gain amplifier whose gain is also controlled by the control processor. The signal is then routed through or around a lock-in amplifier. An analog switching circuit selects either the original signal or lock-in output depending on whether the FIR signal was unchopped (scanning mode) or chopped (position mode), respectively. This signal is then output to an analog tape recorder as well as being sent to an analog-to-digital converter. The digital signal is sent to both the control and display processors. The control processor sends the digital data and additional control information to a serial data port so that it can be recorded on a digital tape recorder. The display processor provides the data to a digital-to-analog converter which provides an analog signal to drive an oscilloscope display which can be monitored by the operator.

The data sampling system is used to determine the times to sample data. Equal intervals of path difference are sensed and trigger sampling when the interferometer is scanned, and equal intervals of time are used when the

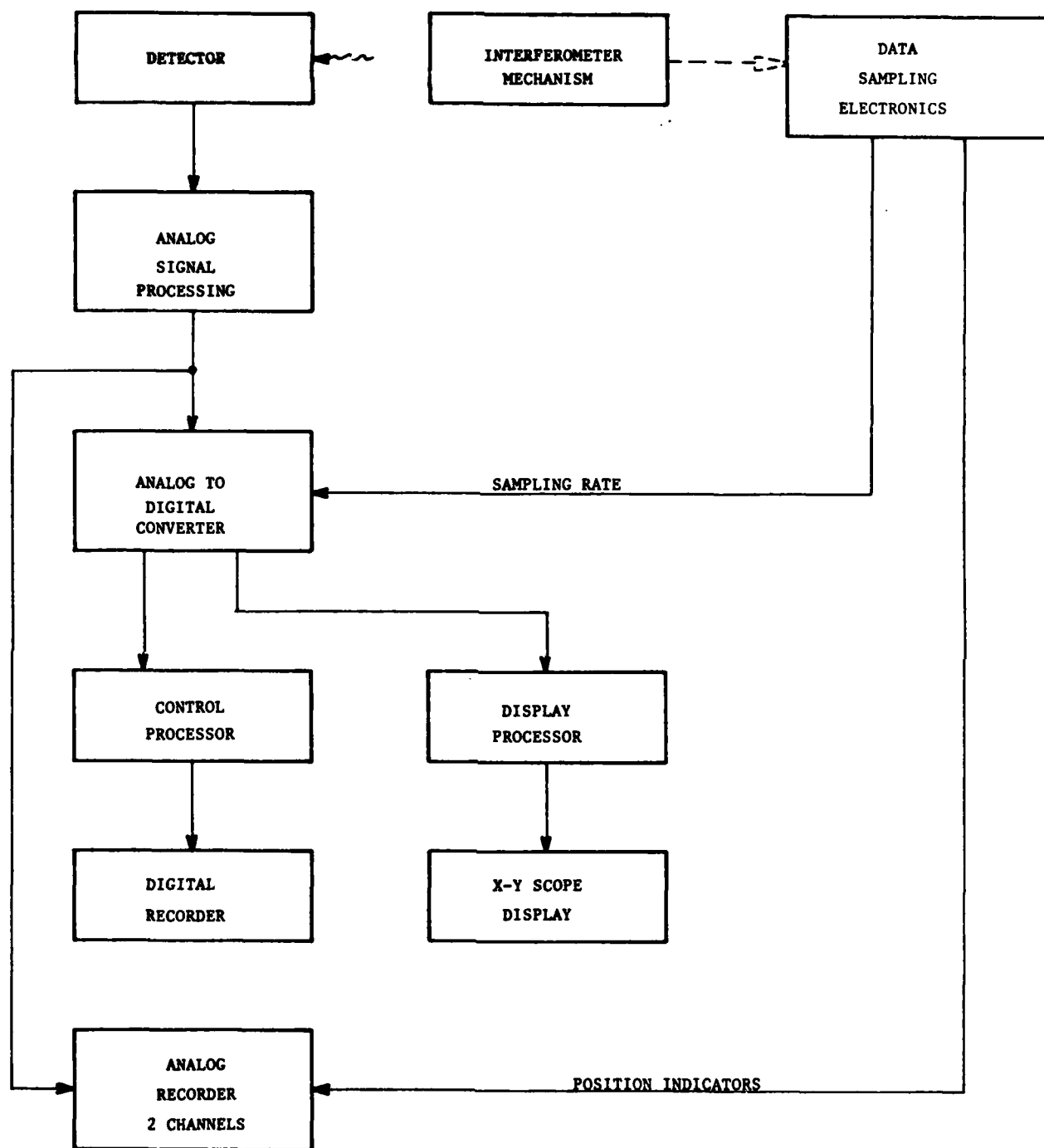


Figure 3.9. Data acquisition systems functional diagram



interferometer is locked in position. While the interferometer is scanned, both encoders (one on each mirror carrier) are used to enhance the accuracy of sampling by a method which will be described in a later section. The encoders are commercially made and of the optical grating type. Each encoder comprises (1) a glass slide on which there is a grating printed by photolithography and (2) a reading head. The latter has a light source, a small mask with lines like the grating, and photo-detectors. As the reading head moves, the detected signal is modulated with the period of the grating. Actually there are four masked detecting elements which are offset from each other so that they provide differential and quadrature detection of the grating pattern. The differential pairs offset by half a grating period provide some immunity to light level variations and the quadrature pairs offset by a quarter period permit the direction of motion to be sensed. In addition, there is a separate single fiducial mark on the glass slide which is alongside the grating pattern. This is sensed by a separate detector element to provide a reference mark from which to reckon position. Apart from this, the encoder is essentially incremental.

The period of the grating is 20  $\mu\text{m}$ , and with the conditioning electronics, an electrical pulse can be derived for every 5  $\mu\text{m}$  of motion of the reading head. These interpolated pulses are triggered by the zero-crossings of the two differential channels in quadrature. The accuracy of encoding depends essentially on two factors: (1) the fundamental accuracy of the ruling of the grating, and (2) the accuracy with which mechanical and electrical adjustments can be made to achieve both a uniform duty cycle between zero-crossings and the phasing between the channels nominally in quadrature. In practice, the latter controls

the accuracy achievable, and the manufacturer estimates that this is about  $\pm 2 \mu\text{m}$ . At  $\pm \lambda/80$  for the shortest wavelength of interest, this degree of accuracy is believed adequate.

#### 4.0 PROBLEMS ENCOUNTERED

The FIRRS instrument package is in almost all aspects representative of the state-of-the-art in far infrared radiometry, and naturally some problems arose in the course of its development. The following sections give brief summaries of some of these, and in the main, significant achievements were made in overcoming the difficulties.

##### 4.1 Bearings

Initially, plans were made to use in the FIRRS interferometer a type of torsional pivot that was similar to that used by AFGL but was more flexible. A simplified analysis suggested that these units were suitable in terms of their strength and angular range. Pivots of this type were purchased and installed, but in the course of testing, several difficulties or failures were encountered which led to their abandonment. First, it was found that the torsional pivots were not strong enough to prevent the armature from clamping against the field. Of course, if the armature were perfectly centered in the field there would be no force on the pivot near the torque motor, but as a practical matter it is not possible to achieve this accurately. The solution was to substitute jewelled bearings and stainless steel pivots for the connection between the rear lever  $\ell_2$  and the interferometer base. The bearing cases and the pivots were made at GT/EES, and the tolerance on the match between the pivot O.D. and bearing I.D. is better than  $2.5 \mu\text{m}$  (or  $10^{-4}$  inch). These bearings were chosen over ball bearings because (1) higher tolerances could be achieved, (2) there would be fewer problems with motion over limited angular deflections as regards wear and smoothness, and (3) it was easier to match the outside dimensions of the torsional pivots. Although there is a noticeable increase in friction with

the jewelled bearings as compared with the torsional pivots, friction is still very low.

After the motor pivot change was made, torsional pivots remained in all the other positions in the interferometer, but three other problems arose with those remaining. Some were susceptible to a resonance vibration at around 20-25 Hz. Others were damaged by the turn-around impulses transmitted through them. Finally, problems were encountered with shifting centers of rotation between the two halves of each torsional pivot when large angular deflections were reached. These effects were too large and inconsistent from one pivot to the next to permit compensation for them. Therefore, all of the torsional pivots were replaced with jewelled bearings and stainless steel pivots, and excellent performance (for these wavelengths) has been achieved.

#### 4.2 Alignment and Stress in a Double-Beam, Push-Pull Interferometer

The GT/EES interferometer design imposes some special mechanical constraints due to the incorporation of two moving mirrors, constraints that were not so severe in previous designs [13] in which only one mirror was moved. If one tries to assemble the scanning mechanism without making allowance for possible imperfections in machining the parts, a bearing/pivot set might not fit in the last joint or might be seriously strained. To alleviate this it is necessary to have some adjustment in the length of at least one of the levers or mirror carriers. However, this is not necessarily satisfactory since the assembled parts may not then form a parallelogram. Parallelograms can be obtained on both sides of the drive if an adjustment can be made in the length of both mirror carriers and of both sides of the lever  $l_2$ . The adjustment in each case is made by moving the hole in which

the bearing or pivot fits. This hole is made to be the inner hole of two nested collets which are slightly eccentric. The eccentricity is a few thousandths of an inch and was made to be nearly identical in the two collets. By rotating the collets with respect to the mirror carrier or lever in which they are mounted, one can move the center line of the hole. When a position is selected, the bearing or pivot is clamped by tightening a screw across a split in the end of the mirror carrier or lever  $\ell_2$ . These adjustments are made while a visible laser beam is reflected from each moving mirror. A check is made that the reflected beam comes back on itself over a long baseline regardless of the angle of the levers, and that there is minimal mechanical stress.

Other steps in the alignment are (1) alignment of the encoder grating lines with the moving mirror surfaces (as well as other optical and electrical adjustments in the encoders), (2) adjustment of the tilts of the folding mirrors M1 and M2 (Figure 3.4) to bring the two reflected interferometer beams into coincidence, and (3) adjustment of the orientation of the polarizing beam dividers as regards the angle of polarization and the tilt of the surface. Steps (2) and (3) are performed with a visible laser, and it was interesting to find that diffraction from the grid polarizers was not confusing but rather served to help define the plane of polarization of each beam divider. Details of alignment procedures are given in [2] and [3].

The overall performance achieved is excellent. The maximum uncorrelated angular difference in the reflected radiation from the two mirrors is about 1.5 mrad. Moreover, for radiation in the band 5 to 30  $\text{cm}^{-1}$ , the depth of modulation at zero path difference was found to be 96 percent of the theoretical maximum.

#### 4.3 Use of Two Parallel Position Encoders to Produce a Combined Position Output Signal

Although the two mirrors in the interferometer are linked mechanically and the motion of either mirror should give an increment of path difference identical to that given by the other, a separate encoder is associated with each as a precaution against the possibility that the two mirrors might have slight but interferometrically significant differences in motion. Each encoder has a resolution and accuracy adequate to measure the translation of the corresponding mirror, as mentioned above. However, it is not straightforward to obtain the sum of the displacements of the two mirrors in order to derive the optical path difference in the interferometer. (Here, the two mirrors are taken to have opposite directions of positive displacement.) If the resolution of the encoders were an order of magnitude more, it would make sense merely to add the counts from the two channels. Since the resolution, however, is near the accuracy needed, the fact that the two encoders will not index (i.e. emit pulses from differential signal zero-crossings) in synchronization defeats any advantage in using two encoders (assuming that the distortions one is trying to compensate are not significantly larger than the resolution of one encoder).

To meet the need for more accurate summing, a circuit was devised that takes from each encoder the cosine-like signal produced by one of its differential detector pairs and multiplies these modulations together. The product signal has a high frequency component whose phase advances with the sum of the displacements, but it also has low frequency components related to the difference in the phases from the two encoders. The low frequency component is removed by a high-pass filtering scheme. This leaves the desired signal, the zero-crossings of which can be used as improved triggers for data sampling.

These occur once every 5  $\mu\text{m}$  in the displacement of one of the mirrors. For simplicity, a quadrature signal has not been derived, as the direction of motion can be obtained from the outputs of one of the encoders and need not be obtained from the product signal.

It should be mentioned that signals from only one of the two encoders are used to control the torque motor. The combined signal from the two encoders is only used to control data logging. The reason for this is that the combined signal is interrupted during the turn-around phase between scans because the high-pass filter defeats it. It is felt that this separation of encoder functions gives both good motor control and good data logging control.

#### 4.4 Other Problems Encountered

Several other topics were mentioned and discussed in previous sections; for example,

- (1) Commercial polarizing beam dividers were found to have inadequate performance for field use. The theory of the performance of polarizing beam dividers is inadequate. Fabrication by photolithography was made more difficult by gases evolved from the photoresist. Solutions to these problems were covered in Section 3.1.
- (2) It was found to be impractical to make double-half-wave filters for use as narrowband optical filters, but improved techniques in the fabrication of alternative Fabry-Perot type filters allowed the design goals to be reached as described in Section 3.4.1.
- (3) Difficulties in making adequate capacitive meshes prevented success in making optical lowpass filters of the interferometric type, but alternative crystal filters met the most important needs, as discussed

in Section 3.4.2.

Further consideration of the difficulties encountered will be given in the context of the overall program in the concluding section.



## 5.0 ACHIEVEMENTS

In the course of the development of the FIRRS instrument package, the state-of-the-art has been advanced in a number of areas. Several achievements have been mentioned in previous sections and the following is a list of most of them:

- (1) An interferometer has been made with exceptionally high interferometric efficiency (96%). This can be attributed to the Martin-Puplett type design and the quality of the beam dividers and of the drive mechanism.
- (2) Beam dividers have been made photolithographically and give excellent performance with much improved ruggedness.
- (3) A careful review of the theory of polarizing beam dividers has been made and compared with observation. Significant discrepancies were found, but a regime in which good performance occurs has been identified.
- (4) Techniques for fabricating Fabry-Perot filters have been improved so that very high transmissions have been achieved at band center for narrowband optical filters.
- (5) Data have been extended into the submillimeter wavelength region for standard microwave absorbing compounds. This has made possible the design of compact thermal calibration sources similar to those used in infrared research by AFGL and others.
- (6) A method has been devised to combine the outputs of two grating type position encoders so that the effect of moving both mirrors in the two-beam interferometer could be monitored. This was a key requirement in a practical high resolution interferometer of this type.

- (7) Background radiation from optical elements was greatly reduced by the use of a small, thin window at the back of the receiving telescope. However, this imposed a requirement for a sealed telescope that was nevertheless shock absorbing. Although as yet untested, the basic design in which the telescope is imbedded in shock absorbing material is believed to be a good solution.
- (8) A design for the optical train was developed that further minimizes background radiation. Key features are the use of Winston cone condensers at the detectors and the placement near the moving interferometer mirrors of the pupil corresponding to the input aperture of the "eyeball" in front of the telescope.

## 6.0 CONCLUSIONS

The makings of a powerful far infrared research facility have been provided. Most aspects of the fabrication and testing of the FIRRS have been completed, but some work remains before it can be deployed, as has been reported in project status reports. In addition to the difficulties encountered in advancing the state-of-the-art, which have been described above, there were difficulties in two other areas which absorbed more time than anticipated in the contract. One was in meeting all the requirements for compatibility between FIRRS and the AFGL flying laboratory. The other was in the development and testing of the microprocessors and related electronic systems. Partly in response to the compatibility requirements, the electronic systems have become quite complex and have required considerable effort to iron out difficulties. Almost all known problems have been overcome, but due to time and financial limitations of the contract, work has stopped short of solving all of them and short of a full system test. Reference may be made to Table 6.1 for details of the current status of the FIRRS instrumentation. Nevertheless, the state-of-the-art in far infrared radiometry has been advanced, and it is hoped that there will one day be the opportunity to fully realize this progress, whether in the present instrument or its successors.

Table 6.1. Status of FIRRS

<u>Module</u>	<u>Status</u>
Telescope	Complete and optically tested
Television Subsystem	Complete and tested (as per Status Report #7)
Calibration Sources	Complete and electrically tested - materials optically tested - not tested with the detectors, but no problems expected
Optical Elements other than those in the Telescope - windows, lens beamsplitters, mirrors	Complete, functionally tested and aligned
Filters	Three out of four narrowband filters perform satisfactorily - transmission too low in fourth. Detector filters are currently a composite dielectric filter. Low-pass interference filters not yet satisfactory.
Interferometer (mechanical and optical parts)	Complete and tested
Detector	Complete and partially tested - all components appear to be operational but final sensitivity and calibration test remain.
Pumping Station	Complete and tested - (per Status Report #7) not tested with the detector
Electronics and Programming	Essentially complete (except for minor program and circuit changes) - some testing remains - problems remaining are noted below.
Known problems remaining in electronics and programming:	<ol style="list-style-type: none"> <li>1) A/D Converter not enabled on retrace.</li> <li>2) No latches on Remote Display.</li> <li>3) Pulse Period Alarm must be tested, then this used to test further the data taking pulse stream.</li> <li>4) Further ruggedness of the electronics appears to be necessary.</li> <li>5) Some of the above may necessitate minor programming changes.</li> </ol>

#### 7.0 ACKNOWLEDGEMENTS

The authors would like to express their appreciation to Dr. Roger Hildebrand and his colleagues at the University of Chicago for cooperation in providing assistance with the fabrication of the Winston cones used in the detector. Thanks are also due to Dr. Sid Perkowitz and the Department of Physics of Emory University for providing the loan of equipment used in the optical evaluation of some of the components of FIRRS. Finally, the authors' appreciation is expressed to Dr. J.H. Schummers and Mr. John Rex of AFGL for their technical suggestions during the program.

## 8.0 REFERENCES

1. R.A. Bohlander, A. McSweeney, D.O. Gallentine, M.J. Sinclair, J.H. Rainwater, and O.A. Simpson, "Far Infrared Radiometric Spectrometer (FIRRS) To Survey Up-Welling Radiation", Phase I Preliminary Design Report, GT/Project A-2519, Contract No. F19628-80-C-0031, U.S. Air Force Geophysics Laboratory (5 June 1980).
2. R.A. Bohlander, J.W. Larsen, D.R. Lamm, M.J. Sinclair, G.D. Holah, A. McSweeney, O.A. Simpson, P.B. Reinhart, and D.O. Gallentine, "Far Infrared Radiometric Spectrometer (FIRRS)", R & D Design and Evaluation Report, GT-Project A-2519, Contract No. F19628-80-C-0031, U.S. Air Force Geophysics Laboratory (30 May 1983).
3. R.A. Bohlander, D.R. Lamm, J.W. Larsen, and M.J. Sinclair, "Far Infrared Radiometric Spectrometer (FIRRS)", Draft Report GT/Project A-2519, Contract No. F19628-80-C-0031, U.S. Air Force Geophysics Laboratory (30 May 1983).
4. S.M. Kulpa and E.A. Brown, Near Millimeter Wave Technology Base Study. Volume I. Propagation and Target Background Characteristics. Report for U.S. Army Material Development and Readiness Command and the Defense Advanced Research Projects Agency, Harry Diamond Laboratories Report HDL-SR-79-8 (1979).
5. J.J. Gallagher, R.W. McMillan, and R.G. Shackelford, "Military Systems Applications at Near-Millimeter Wavelengths", SPIE 197, 170-190 (1979).
6. J.J. Gallagher, P.B. Reinhardt, R.W. McMillan, and J.H. Rainwater, "The Investigation of the Feasibility of Airborne Detection of Submillimeter Missile Plume Radiation", Final Technical Report for Contract No. DASG060-78-C-0031, Ballistic Missile Defense Advanced Technology Center, February 22, 1979.
7. V.J. Falcone and L.W. Abreu, "Millimeter Wave Propagation Modeling", SPIE 259, 58-66 (1980).
8. R.W. Saunders, Ph.D. Thesis, University of London (1979).
9. R. Hinder and M. Ryle, Mon. Not. R. astr. Soc. 154, 229-253 (1971).

10. A.J. Kemp, IV Intl. Conf. Infrared and Millimeter Waves and their Applications, sponsored by IEEE, Miami Beach, FL, December 10-15, 1979, Digest pp. 173-174.
11. J.J. Gallagher, J.H. Rainwater, (private communication).
12. D.H. Martin and E. Puplett, Infrared Physics 10, 105ff (1969).
13. R.P. Walker and J.D. Rex, "Interferometer design and data handling in a high vibration environment. Part I: interferometer design"; and J.H. Schummers, "... Part II: data handling" SPIE 191, 88-91, 92-95 (1979).
14. G.D. Holah, "Far-Infrared and Submillimeter-Wavelength Filters", in Infrared and Millimeter Waves, ed. K. Button, Vol. 6, Chapt. 6, New York: Academic Press (1982).
15. G.D. Holah, B. Davis, and N.D. Morrison, "Narrow-Bandpass Filters for the Far-Infrared using Double-Half-Wave Designs", Infrared Physics 19, 639-647 (1979).
16. R. Iwasaki, "Microwave Blackbody Radiometer Calibration Standards", Millimeter Wave Workshop, NELC, November, 1976.
17. M.D. Blue, S. Perkowitz, IEEE Trans. MTT-25, 491-493 (1977).
18. O.A. Simpson, B.L. Bean, S. Perkowitz, J. Opt. Soc. Am. 69, 1723-1726 (1979).
19. D.A. Harper, R.H. Hildebrand, R. Stiening, and R. Winston, "Heat trap: an optimized far infrared field optics system", Appl. Opt. 15, 53-60 (1976).

